Wall modeling for large-eddy simulation using an immersed boundary method

By F. Tessicini †, G. Iaccarino, M. Fatica, M. Wang AND R. Verzicco ‡

1. Motivation and objectives

Orthogonal, structured grids allow flow simulations in simple geometries with high efficiency and accuracy. In contrast, complex and realistic flow problems have traditionally required the use of curvilinear or unstructured meshes, which require large computational costs and reduced accuracy due to limited grid smoothness and orthogonality. In recent years an alternative approach which combines the advantages of simple Cartesian grids with the ability to deal with complex geometries has been developed. In this technique, named the immersed boundary method (Fadlun *et al.* (1999)), the complex object is *immersed* in a regular grid and the body effect on the flow is accounted for by prescribing an appropriate body force in the momentum equations in the first computational cell outside the immersed body. This is a *de facto* grid-free numerical method in the sense that the time-consuming construction of the smooth mesh fitted to the body is avoided.

Flows in industrially relevant configurations are often characterized by high Reynolds numbers. A Direct Numerical Simulation (DNS) which resolves all the time and length scales requires grid resolution and computational resources that will not be available in the near future. Turbulence models have to be used to make those simulations feasible. The immersed boundary approach has been used successfully in combination with Large-Eddy Simulation (LES) and Reynolds Averaged Navier-Stokes (RANS) techniques (Iaccarino & Verzicco (2003)). Accurate LES of wall bounded flows, however, requires a near-wall resolution comparable to that for DNS, thus limiting the use of LES to moderate Reynolds numbers. One way to overcome this difficulty is to replace the near-wall region with a wall model which provides the outer LES with approximate wall boundary conditions. In recent years wall models based on turbulent boundary-layer equations and their simplified forms (Balaras, Benocci & Piomelli (1996); Cabot & Moin (2000); Wang & Moin (2002)) have been developed and applied successfully in a number of flow configurations.

The objective of this work is to study the applicability of a simple near-wall model, based on the local equilibrium hypothesis, in the framework of immersed boundary method for LES and to analyze its effect on the flow dynamics. The selected test case is the flow past a 25 degree, asymmetric trailing edge of a model hydrofoil. The Reynolds number based on free-stream velocity U_∞ and the hydrofoil chord C, is $Re_C = 2.15 \times 10^6$. The simulation is performed over the rear 38% of the hydrofoil chord, and the Reynolds number based on the hydrofoil thickness is $Re = 1.02 \times 10^5$. The flow was investigated experimentally by Blake (1975) and numerically by Wang & Moin (2000), who reported that 200 CRAY C-90 CPU hours were needed to advance the simulation by one flow-through time for a fully resolved LES.

† DMA, Università di Roma La Sapienza, Via Eudossiana, 18, 00184, Roma, Italy. Also with INSEAN, Via di Vallerano 139, 00128, Roma, Italy.
‡ DIMeG and CEMeC, Politecnico di Bari Via Re David, 200, 70125, Bari, Italy.

2. Numerical set-up and wall model

The equations used for the present study are the three-dimensional, incompressible, unsteady Navier-Stokes equations with an additional boundary body-force term $\mathbf{f}$:

$$\frac{D\overline{\mathbf{u}}}{Dt} = -\rho^{-1}\nabla\overline{P} + \nabla\cdot\{\tilde{\nu}[\nabla\overline{\mathbf{u}} + (\nabla\overline{\mathbf{u}})^T]\} + \mathbf{f}\ , \tag{2.1}$$

$$\nabla\cdot\overline{\mathbf{u}} = 0\ . \tag{2.2}$$

Here $\overline{\mathbf{u}}$ denotes the filtered velocity, and $\overline{P}$ is the sum of the filtered pressure and the trace of the subgrid-scale stress tensor. The effective viscosity $\tilde{\nu}$ is the sum of the subgrid-scale eddy viscosity and the molecular kinematic viscosity. The subgrid-scale turbulent viscosity is determined by a dynamic procedure and does not require direct specification of any model constant (Germano *et al.* (1991); Lilly (1992)).

The equations are solved by a second-order centered finite-difference solver. Details on the numerical methods and on the expression for $\mathbf{f}$ are given in Fadlun *et al.* (1999). Here it suffices to mention that if the time-discretized version of (2.1) is

$$\overline{\mathbf{u}}^{n+1} - \overline{\mathbf{u}}^{n} = \Delta t(RHS + \mathbf{f})\ , \tag{2.3}$$

(with Δt the computational time step and RHS the sum of nonlinear, pressure, and viscous terms), to impose $\overline{\mathbf{u}}^{n+1} = \overline{\mathbf{v}}_b$, the boundary velocity, the body force $\mathbf{f}$ must be,

$$\mathbf{f} = -RHS + \frac{\overline{\mathbf{v}}_b - \overline{\mathbf{u}}^{n}}{\Delta t}. \tag{2.4}$$

This forcing is active only in the flow region where we wish to mimic the solid body, and it is set to zero elsewhere. In general, the surface of the region where $\overline{\mathbf{u}}^{n+1} = \overline{\mathbf{v}}_b$ does not coincide with a coordinate surface, therefore the value of $\mathbf{f}$ at the node closest to the surface but outside the solid body is linearly interpolated between the value yielding $\overline{\mathbf{v}}_b$ on the solid body and zero in the flow domain. This interpolation procedure is consistent with a centered second-order finite-difference approximation, and the overall accuracy of the scheme remains second-order. The linear interpolation, however, can be used only if the location of this point is inside the linear region of the boundary layer. In order to extend the applicability of the immersed boundary method to higher Reynolds number flows, a two-layer wall modeling approach will be considered instead of the linear interpolation.

Equations (2.1) and (2.2) are solved down to the second grid point from the solid boundaries. From the second grid point to the wall a refined mesh is embedded, and simplified turbulent boundary-layer equations are solved. The boundary-layer equations have the following general form (Balaras, Benocci & Piomelli (1996); Wang & Moin (2002)):

$$\frac{\partial}{\partial x_n}\left[(\nu+\nu_t)\frac{\partial\overline{u}_i}{\partial x_n}\right] = F_i, \qquad \text{with}$$

$$F_i = \frac{\partial\overline{u}_i}{\partial t} + \frac{\partial\overline{u}_i\overline{u}_j}{\partial x_j} + \frac{\partial\overline{p}}{\partial x_i}, \tag{2.5}$$

where n denotes the direction normal to the wall and $i = 1, 3$ the wall parallel directions. In the present study only a simplified version of the above model, namely the equilibrium stress balance model obtained by setting $F_i = 0$ in (2.5), was used. The eddy viscosity ν_t is obtained from a simple mixing length eddy viscosity model with near wall damping

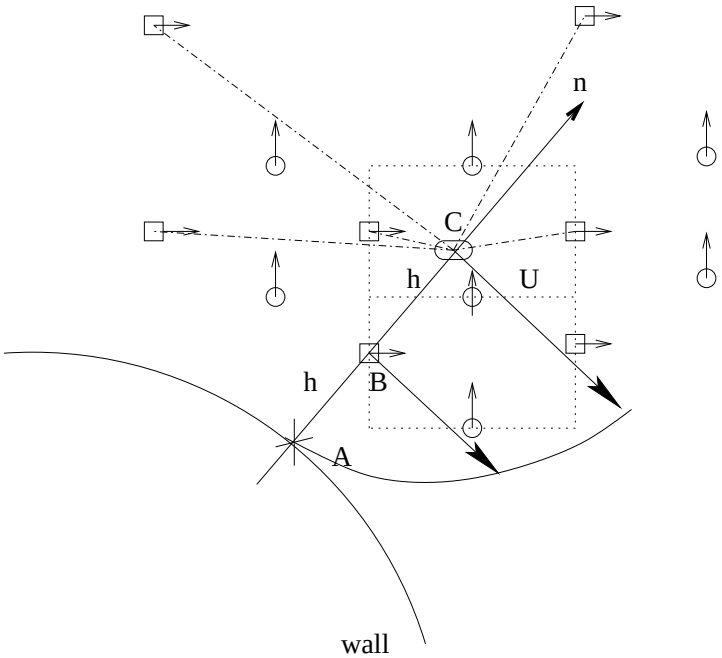

FIGURE 1. Interpolation procedure: ▫ , streamwise velocity node; ∘ , vertical velocity node. n is normal to the wall from first external point B. U is the tangential velocity interpolated at point C, used as boundary condition for the wall model.

(Cabot & Moin 2000; Wang 2002)

$$\frac{\nu_t}{\nu} = \kappa y^+ (1 - e^{-\frac{y^+}{A}})^2, \tag{2.6}$$

where y^+ is the distance to the wall in wall units based on the the local instantaneous friction velocity, $\kappa = 0.4$, and $A = 19$. The boundary conditions for the wall model are the LES velocities at the outer edge of the wall-layer and the no-slip condition at $y = 0$. Since in (2.6) the friction velocity u_τ is required to determine y^+ which, in turn, depends on the wall shear stress given by (2.5), an iterative procedure has been implemented to solve (2.5) and (2.6) simultaneously. It is worth mentioning that for a general geometry, an interpolation procedure is needed for the calculation of the tangential velocity in (2.5) since the wall normal does not cross any computational node. The choice of the interpolation points follows the approach used by Balaras (personal communication): all the first external grid nodes are identified, the wall normals are drawn through these points, and the interpolation node is placed on the same segments at twice the distance h (see figure 1). The choice of $2h$ is somewhat arbitrary but, as noted by Balaras, it allows the most compact scheme without involving points inside the body. The fluid velocity at the interpolation point is computed using the inverse distance formula based on the grid points surrounding the interpolation node.

The computational cost of the wall model, including the interpolation procedure, is about 10% of the total computational cost.

The equilibrium stress balance model implies the logarithmic law of the wall for instantaneous velocity at $y^+ \gg 1$ and linear velocity for $y^+ \ll 1$. Figure 2 shows the velocity profiles given by the model when it is used in the low ($Re = 300$) and higher

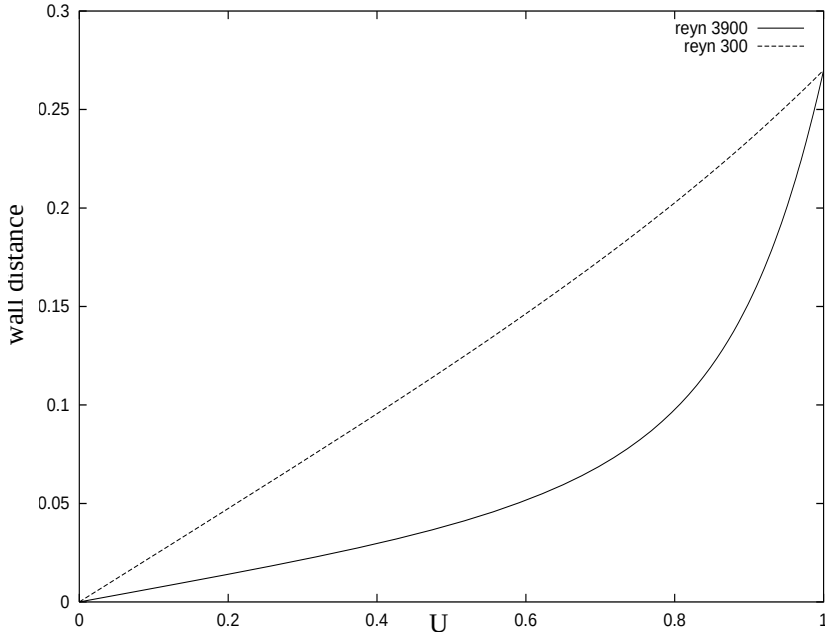

FIGURE 2. Velocity profiles as a function of wall-normal distance, as predicted by (2.5) and (2.6) at two different Reynolds numbers.

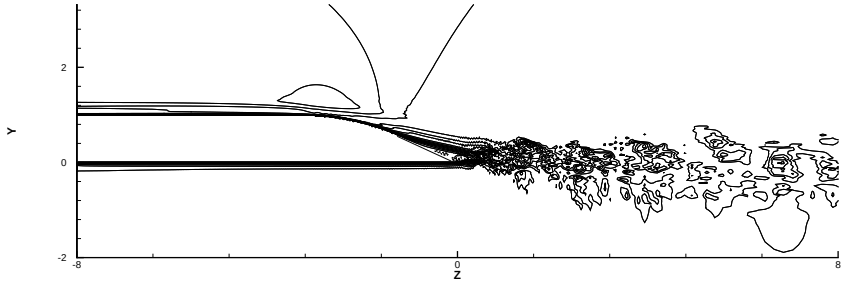

FIGURE 3. Flow past a hydrofoil trailing edge. The contours (−0.2 to 1.2 with increment 0.08) represent the instantaneous streamwise velocity.

($Re = 3900$) Reynolds number cases. In the former case the first interpolation node is located at $y^+ = 5$, while in the latter it is at $y^+ = 30$. It can be observed that the linear interpolation usually adopted in immersed boundary procedures is automatically recovered when the first external node is located in the viscous sublayer of the turbulent boundary layer. In contrast, when the interpolating node is within the log layer, the wall model yields the appropriate velocity profile thus extending the range of applicability of the immersed boundary method in conjunction with LES to the high Reynolds-number regime.

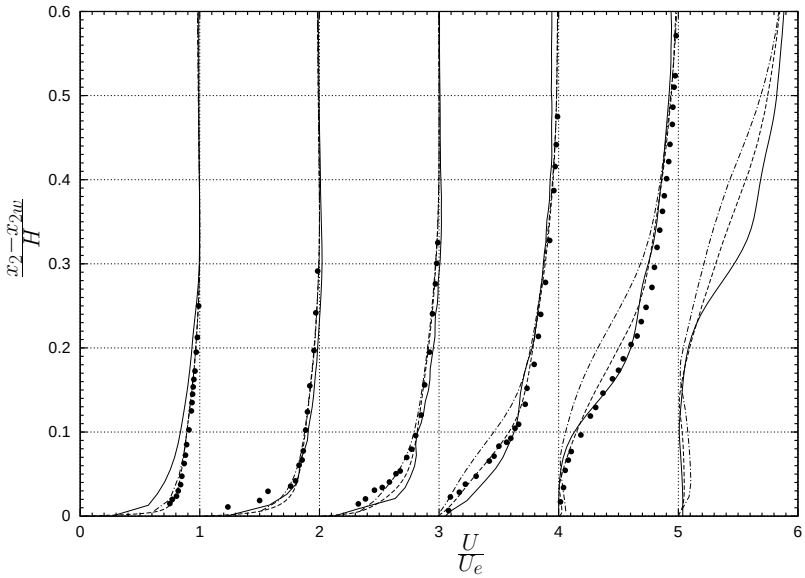

FIGURE 4. Mean velocity magnitude at (from left to right) $x_1/H = -3.125$, -2.125, -1.625, -0.625, 0. •, experiment (Blake 1975); – – – –, full LES (Wang & Moin 2000); ———, present calculation; —·—, LES with wall model (Wang & Moin 2002).

3. Preliminary results and discussion

In the simulation with the wall model the computational domain is $0.25H \times 41H \times 16.5H$, where H denotes the hydrofoil thickness. The grid has $25 \times 206 \times 418$ points, respectively, in the spanwise, cross-stream and streamwise directions. The grid distributions of the Cartesian mesh in the cross-stream and streamwise directions are the same as that used by Wang & Moin (2002) for the straight part of the profile. A uniform mesh with $0.013H$ spacing is used between the upper and lower sides of the hydrofoil in the cross-stream direction. The mesh is uniform in the spanwise direction and non-uniform in the other directions, with nodes clustered around the wall and near the trailing edge in the wake. The distance in wall units from the second off-wall grid point (where the wall model is required to match the local LES velocity) to the wall is in the straight portion of the hydrofoil about $\Delta x_2^+ = 120$. Compared to the full LES performed by Wang & Moin (2000), this simulation has a spanwise domain width that is half of the original one.

In figure 4 the mean velocity magnitude computed using the immersed-boundary technique with wall modeling is compared with the experimental (Blake 1975) and full LES (Wang & Moin 2000) data. Result from the LES of Wang & Moin (2002) on a body-fitted mesh with the same equilibrium stress-balance model is also plotted for reference. The velocity magnitude, defined as $U = (U_1^2 + U_2^2)^{\frac{1}{2}}$, is normalized by its value U_e at the boundary layer edge. The vertical coordinate is measured as the vertical distance to the upper surface. Although considerable discrepancies exist with the experimental and full LES results, compared to the simulation without wall model on the same grid (figure 5), the improvement is evident.

The largest deviation between the present predictions and the full LES solution occurs at $x_1/H = -1.625$ where the second off-wall grid point, used as outer boundary for the wall model, is far from the wall. The location of the outer-boundary for the wall model (first off-wall LES grid point in Wang and Moin (2002) *vs.* second off-wall point in the

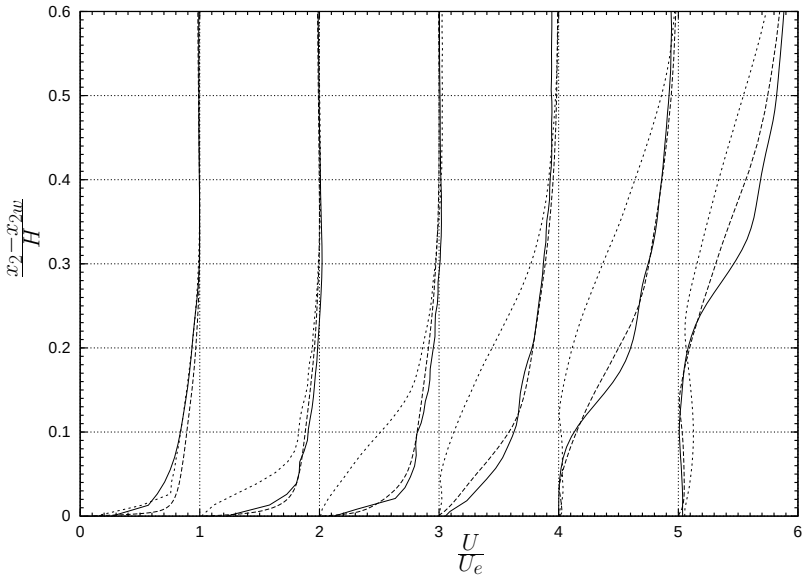

FIGURE 5. Mean velocity magnitude at (from left to right) $x_1/H = -3.125$, -2.125, -1.625, -0.625, 0. - - - - , full LES (Wang & Moin 2000); ——— , present LES with wall model; — — — , present LES without wall model.

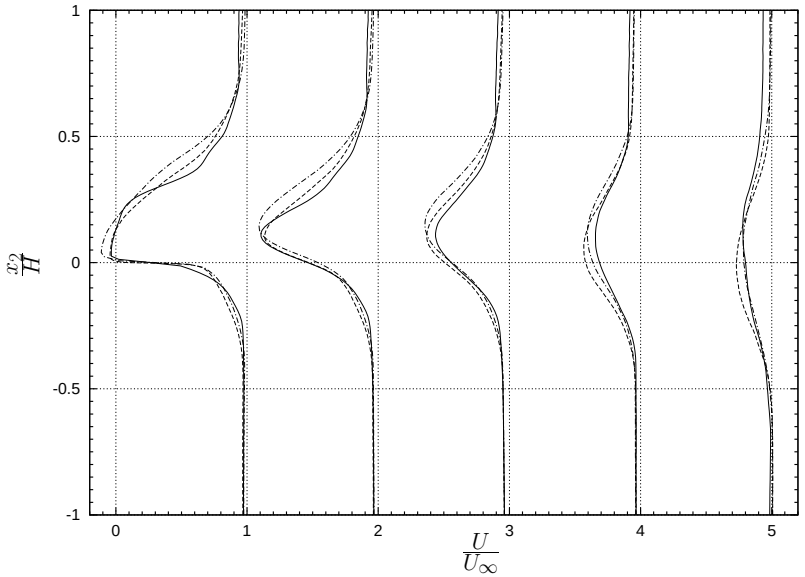

FIGURE 6. Profiles of the normalized mean streamwise velocity in the wake, at (from left to right) $x_1/H = 0$, 0.5, 1.0, 2.0, 4.0. - - - - , full LES (Wang & Moin 2000); ——— , present calculation; —·— LES with wall model (Wang & Moin 2002).

present work) constitutes a major difference between the present model implementation and that of Wang & Moin. This could be the cause for the observed discrepancies between the two wall model solutions, and a grid refinement study in the cross-stream direction is needed to test the sensitivity of the wall model to the outer boundary location. It is noted that the present simulation predicts the separation point near the trailing edge

quite well but a strong deviation from the full LES is observed in the upper part of the trailing-edge station $x_1/H = 0$, possibly due to the small spanwise dimension. As pointed out by Wang & Moin (2002), their spanwise domain size, at half the hydrofoil thickness, was too small. In the present simulation it is even smaller by another 50%. New simulations are underway in order to rectify the above deficiencies and to test the capability of the method to compute the turbulent stresses. Finally, figure 6 depicts the wake profiles in terms of the mean streamwise velocity, which show reasonable agreement with the full LES and previous wall modeling results.

4. Acknowledgments

Fabrizio Tessicini has been partially supported by the Ministero delle Infrastrutture e dei Trasporti in the framework of the INSEAN research plan 2000-2002.

REFERENCES

Balaras, E., Benocci, C., Piomelli, U. 1996 Two-layer approximate boundary conditions for large-eddy simulations. *AIAA J.* **34**, 1111–1119.

Blake, W.K. 1975 *A Statistical Description of Pressure and Velocity Fields at the Trailing-Edge of a Flat Structure.* DTNSRDC Report 4241, David Taylor Naval Ship R. & D. Center, Berthesda, Maryland.

Cabot, W. & Moin, P. 2000 Approximate wall boundary conditions in the large-eddy simulation of high Reynolds number flow. *Flow Turb. Combust.* **63**, 269-291.

Fadlun, E.A., Verzicco, R., Orlandi, P. & Mohd-Yusof, J. 1999 Combined immersed-boundary finite difference methods for three-dimensional complex flow simulations. *J. Comp. Phys.* **161**, 35-60.

Germano, M., Piomelli, U., Moin, P. & Cabot, W.H. 1991 A dynamic subgrid-scale eddy viscosity model. *Phys. Fluids A* **3**, 1760-1765.

Iaccarino, G & Verzicco R. 2003 Immersed boundary technique for turbulent flow simulations. To appear in *Applied Mech. Rev.*

Lilly, D.K. 1992 A proposed modification of the Germano subgrid-scale closure method. *Phys. Fluids A* **4**, 633-635.

Wang, M., & Moin, P. 2000 Computation of trailing-edge flow and noise using large-eddy simulation. *AIAA J.* **38**, 2201-2209.

Wang, M. & Moin, P. 2002 Dynamic wall modeling for LES of complex turbulent flows. *Phys. Fluids* **14**, 2043-2051.